Research Article Open Access

Rezene Mahatsente*

Plate Coupling Mechanism of the Central Andes Subduction: Insight from Gravity Model

https://doi.org/10.1515/jogs-2019-0002
Received November 7, 2018; accepted January 25, 2019

Abstract: The Central Andes experienced major earthquake (Mw =8.2) in April 2014 in a region where the giant 1877 earthquake (Mw=8.8) occurred. The 2014 Iquique earthquake did not break the entire seismic gap zones as previously predicted. Geodetic and seismological observations indicate a highly coupled plate interface. To assess the locking mechanism of plate interfaces beneath Central Andes, a 2.5-D gravity model of the crust and upper mantle structure of the central segment of the subduction zone was developed based on terrestrial and satellite gravity data from the LAGEOS, GRACE and GOCE satellite missions. The densities and major structures of the gravity model are constrained by velocity models from receiver function and seismic tomography.

The gravity model defined details of crustal and slab structure necessary to understand the cause of megathrust asperity generation. The densities of the upper and lower crust in the fore-arc (2970 – 3000 kg m^{-3}) are much higher than the average density of continental crust. The high density bodies are interpreted as plutonic or ophiolitic structures emplaced onto continental crust. The plutonic or ophiolitic structures may be exerting pressure on the Nazca slab and lock the plate interfaces beneath the Central Andes subduction zone. Thus, normal pressure exerted by high density fore-arc structures and buoyancy force may control plate coupling in the Central Andes. However, this interpretation does not exclude other possible factors controlling plate coupling in the Central Andes. Seafloor roughness and variations in pore-fluid pressure in sediments along subduction channel can affect plate coupling and asperity generation.

Keywords: Andes subduction zone, Gravity modeling, Lithosphere, Plate coupling, Seismicity

***Corresponding Author: Rezene Mahatsente:** Dept. of Geological Sciences, University of Alabama, Tuscaloosa, AL 35487 USA, E-mail: rmahatsente@ua.edu

1 Introduction

The Central Andes subduction zone is a classic example of a mountain-forming convergent zone. The present day structure of the convergent zone is the result of 200 Myr of ongoing Nazca plate subduction beneath the South American continent (e.g. Isacks 1988; Allmendinger et al., 1997; Oncken et al., 2006; Fig. 1). The margin is highly segmented and exhibits along-strike variations in tectonics, subduction angle, volcanism, crustal thinning, crustal age, seismicity, and northward shallowing of slab (Gutscher, et al., 2000; Lallemand et al., 2005; Tassara, 2005; Oncken et al., 2006; Anderson et al., 2007; Moreno et al., 2008, 2009; Bilek, 2010; Moreno et al.,2011).

Large segment of the South American margin is seismically active and has experienced several large magnitude earthquakes (Mw= 8+) during historical time (Bilek, 2010). This is the region where the massive 2010 Maule (Mw = 8.8) earthquake occurred (Rietbrock et al., 2012; Kato and Nakagawa, 2014). The largest earthquake ever recorded in South America is the 1960 Valdivia earthquake (Mw = 9.5). This earthquake caused large tsunamis and slow rupture in the region (Moreno et al., 2008). Also notable is the Antofagasta earthquake, magnitudes 8.1. A significant after-slip was observed after the major Antofagasta earthquake (Moreno, et al., 2008; Rietbrock et al., 2012; Kato and Nakagawa, 2014).

The rupture zones of the recent major earthquakes in the Central Andes (Iquique 2014, Mw=8.2 and Illapel 2015, Mw = 8.3; Li and Ghosh, 2017; Braitenberg and Rabinovich, 2017) are smaller than the rupture zones of major historical earthquakes (Ruiz and Madariaga, 2018). The 2014 Iquique earthquake (Mw=8.2) did not break the entire seismic gap zone as predicted (Ruiz and Madariaga, 2018). Thus, a significant section of the Peru-Chile convergent zone is building up stresses along the seismic gap zones. The region still has a large seismic potential (Schurr et al., 2012). The high interseismic coupling in northern and southern Peru indicates increased elastic energy since the 1746 and 1868 earthquakes of magnitude 8.6 and 8.8, respectively (Chlieh et al., 2011). The seismicity in the northern Chile exhibits similar seismic patterns. The plates below northern Chile are highly coupled (Béjar-Pizarro et al., 2013; Métois et al., 2013). The highly coupled zones in the northern Chile are separated by narrow zones of low coupling (Fig. 2; Chlieh et al., 2011; Béjar-Pizarro et al., 2013; Métois et al., 2013). The 2014 Iquique earthquake (Mw= 8.2) occurred in the narrow zone of low coupling off the coast of Pisagua (Kato and Nakagawa, 2014).

The factors controlling seismic gaps in the Central Andes are not well understood. However, the correlations of oceanic features at the trench with trench-parallel changes in slab geometry suggest that slab configuration may be the main controlling factor of seismic gaps in the Central Andes (Tassara et al., 2006). Several studies suggest northward shallowing of the Nazca slab (Gutscher, et al., 2000; Lallemand et al., 2005; Tassara, 2005; Moreno et al., 2009). The shallow slab may have increased the compressive stress near the trench and contributed to the seismic gaps in the region.

Most of the seismic gaps in this region are well delineated. However, the mechanism of plate coupling and asperity generation (regions of high seismic moment release) is not well understood. Two hypotheses have been suggested to explain the locking mechanism along the slab, which have so far kept the slab from slipping to cause major earthquakes in the region. One possible explanation is that highly buoyant oceanic features undergo subduction, pulling the slab upward into the overlying plate (Bilek et al., 2003; Bilek, 2007; Audin et al., 2008; Álvarez et al., 2014; Bassett and Watts, 2015). The second and equally convincing hypothesis is that high density fore-arc structures and buoyancy forces exert pressure on the subducting slab, locking the interface between the subducting and overriding plates (Delouis et al., 1996; Sobiesiak et al., 2007; Tassara 2010; Schaller et al., 2015). Thus, mass distribution in the fore-arc may control plate coupling. The slip distributions of major earthquakes in the Chilean margin correlate with trench parallel segmentation of vertical gravity gradient, which is attributed to mass distribution after major earthquakes (Álvarez et al., 2017).

Understanding complex relationships between plate coupling and fore-arc structures in the Andes requires detailed knowledge of the crust and upper mantle structure. Existing gravity models in the Central Andes, developed under the framework of collaborative researches (SFB 267, 574 & SPP 1257), show a highly segmented fore-arc (Götze et al., 1994; Schmidt and Götze, 2006; Tassara et al., 2006; Hackney et al., 2006; Prezzi et al., 2009; Gutknecht et al., 2014). In this paper, I assessed the effects of the along-strike crustal segmentation of the overriding South American lithosphere on plate coupling using 2.5-D satellite and terrestrial gravity data modelling. The main goal of this study is three-fold: (1) determine the locking mechanism of the Central Andes subduction zone, (2) establish the link between trench-parallel crustal thickness and density variations and short-term deformation (earthquake), and (3) define details of crustal and slab structures in the subduction zone.

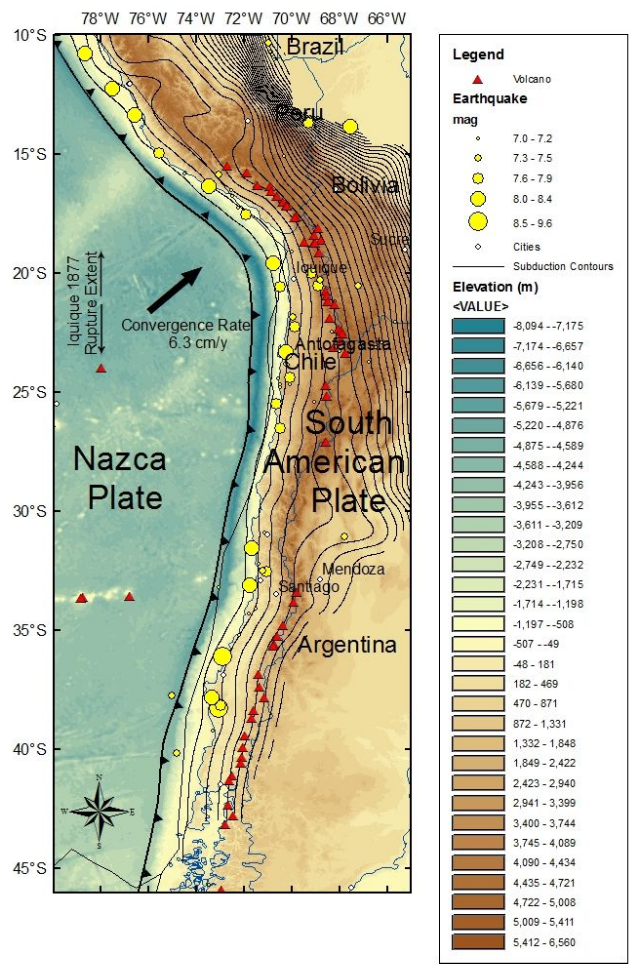

Figure 1: Regional map of the Peru Chile subduction zone. The elevation data are from the National Oceanic and Atmospheric Administration. Black arrow indicates the direction of plate motion. Red triangles are for volcanos. The yellow circles indicate earthquake epicenters (events from 1957 - 2018; USGS Earthquake Archive).

2 Andean Tectonics and Geodynamics

The current structure and configuration of the Andes are the results of three major deformation events that ocurred in the Early Cretaceous, Mid Eocene, and Late Oligocene.

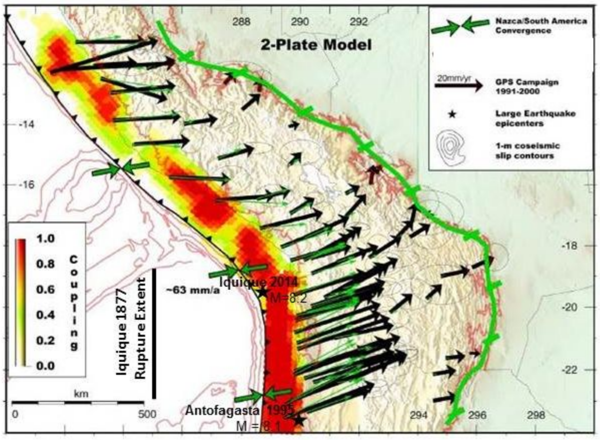

Figure 2: Distribution of interseismic coupling coefficient in the Peru Chile subduction zone. The coefficients are determined based on geodetic data (Chlieh et al., 2011). Black and green arrows are observed and predicted horizontal GPS displacements, respectively.

Most significantly, the Late Oligocene deformation caused the division of the Farallon plate into the Nazca and Cocos plates (Tassara, 2010; Charrier et al., 2013). This latest deformation event caused an increase in the convergence rate between the Nazca plate and the South American plate (Tassara, 2005, 2010; Charrier et al., 2013).

The successive deformation events in the Andes resulted in along-strike segmentation of the convergent zone. Each segment differs in topography, crustal age, volcanism, seismicity, seafloor spreading, and slab configuration (Tassara et al., 2006).

Seismological data indicates northward shallowing of the subducting Nazca slab (cf. e.g. Gutscher, et al., 2000). The flat slab subduction in Peru and south-central Chile has strong effects on the crustal structure of the convergent zone and is one of the controlling factors of plate coupling and asperity generation.

Various hypotheses have been suggested to explain the cause of flat slab subduction in the Andes. The correlation of the subducting Juan Fernandez Ridge with the shallow slab suggests that the buoyancy of the thickened ridge crust may have controlled the style of subduction (Gutscher et al., 2000; Yáñez et al., 2001; Anderson et al., 2007). In addition to the buoyant nature of the Juan Fernandez Ridge, westward motion of the South American plate (Lallemand et al., 2005) and structural segmentation of the overriding South American continental lithosphere have been suggested as factors affecting the present configuration of the slab in the Central Andes subduction zone (Pérez-Gussinyé, et al., 2008).

The Andean convergent zone exhibits along-strike variations in crustal age and volcanism. The region exhibits volcanic gap between the southern and central volcanic zones. The volcanic gap has been developing for 10 Myr and is due to the occurrence of flat sections of the subducting slab at depths between 100 and 150 km (Tassara et al., 2006; Tassara, 2005, 2010). The variations in crustal age are largely associated with fracture zones and oceanic ridges, which cause seafloor spreading and influence slab geometry (Tassara et al., 2006; Bilek, 2010; Tassara, 2010).

3 Gravity Databases

The satellite missions have provided unprecedented gravity and gravity gradient data from extremely low altitude (e.g. 255 km for GOCE mission). Earth gravitational models derived from CHAMP, GRACE and GOCE data provide global gravity field with a spatial resolution of ~ 80 km (e.g. EIGEN-6S Förste et al., 2011; GOCO03S Mayer-Gürr et al., 2012; GOGRAV02S Yi and Rummel, 2013). The resolution becomes much higher (~ 8 km) when satellite-derived gravity data are combined with surface and satellite altimetry-derived gravity data (e.g. EGM2008 Pavlis et al., 2012; EIGEN-6C4 Förste et al., 2014). The gravity data from these missions can be used to fill data gaps in regions where previously no terrestrial gravity data were available. In particular, the gravity gradient tensors from the GOCE mission are unprecedented and add new information to the regional scale lithospheric modelling and interpretation of active convergent margins.

The gravity data used for this study are based on the European Improved Gravity Model of the Earth (EIGEN-6C4; Fig. 3). The EIGEN-6C4 geopotential model is a spherical harmonic representation of the gravitational field of the Earth up to degree and order of 2190 and is based on the WGS84 reference system (Förste et al., 2014). The geopotential model is constrained by terrestrial and satellite gravity data from the LAGEOS (Laser Geodynamics Satellites), GRACE (Gravity Recovery And Climate Experiment) and GOCE (Gravity Field and Steady-State Ocean Circulation Explorer) satellite missions (Förste et al., 2014).

The spatial resolution of the geopotential models (e.g. EGM2008, EIGEN-6C4) depends on the availability of high-quality land gravity data. The resolution is higher where topographic relief is moderate (<3000 m; Koether et al., 2012; Álvarez et al., 2012; Bomfim et al., 2013; Hosse et al., 2014; Gutknecht et al., 2014; Goetze and Pail, 2018).

There are existing land gravity data in the Central Andes, and these data are included in the EGM2008 and

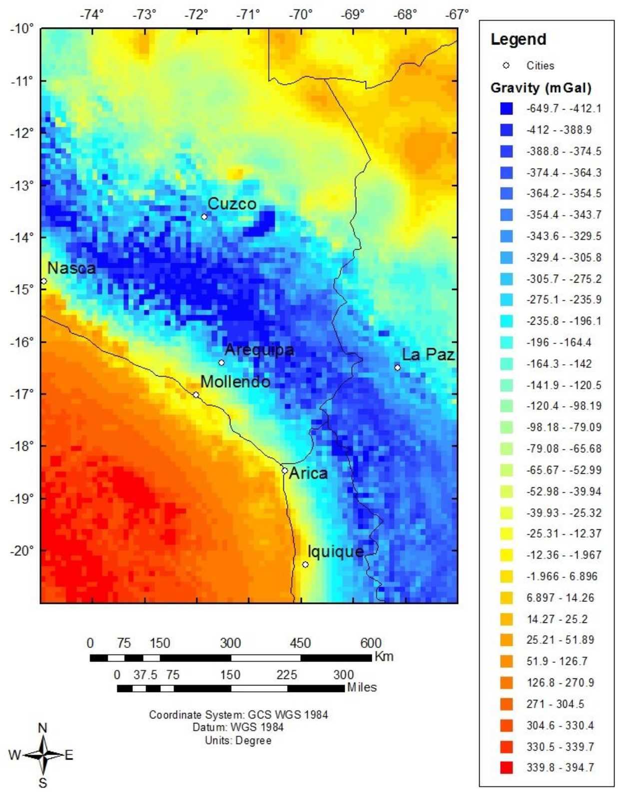

Figure 3: Complete Bouguer anomaly map of the Peru Chile subduction zone. The gravity data are from the EIGEN-6C4 geopotential model that includes terrestrial and satellite-derived gravity data (Förste et al., 2014). The EIGEN-6C4 model has degree and order of 2190 (spatial resolution ca. 8 km).

EIGEN-6C4 models (cf. e.g. Pavlis et al., 2012; Förste et al., 2014).

To develop the 2.5-D gravity models of the Central Andes subduction zone, the free air gravity anomalies of the region (between 67°W/10°S and 75°W/20°S) have been downloaded from the data portal of the International Centre for Global Earth Models (ICGEM: http://icgem.gfz-potsdam.de/ICGEM/). Then, the complete Bouguer anomalies of the Central Andes (Fig. 3) have been computed using Gravity Terrain Correction code, GTeC (Cella, 2015). The GTeC code is based on spherical cap corrections. The complete Bouguer reduction includes curvature and terrain corrections. The code calculates the gravity effect of a rectangular prim for distant zone and a polyhedron for closest zone. The terrain corrections have been applied up to a radius of 168 km. The corrections are based on elevation data from the Shuttle Radar Topography Mission (SRTM; Jarvis et al., 2008) and global relief model of the Earth's surface (ETOPO-1; Amante and Eakins, 2009). The standard reduction density for this study is 2670 kg m^{-3}.

4 Initial Model and Data Constraints

The Central Andes has been the subject of research interest for more than five decades. The results of previous studies in the region (discussed below) have been used to constrain the initial 2.5-D gravity model and reduce the inherent ambiguity in gravity data interpretation.

The densities and geometries of major structures, such as the crust, lithospheric mantle, asthenosphere, and the subducting slab were constrained by velocity models from receiver function and seismic tomography (e.g. Gutscher et al., 2000; Yuan et al., 2000; Husen et al., 2000; Oncken et al., 2003; Krabbenhöft, et al., 2004; Comte et al., 2004). The P-wave velocities of the crust, as determined from seismic refraction-reflection experiments and earthquake tomography, range from 6.5 to 7.3 km s^{-1} in the ocean and from 5.0 to 7.3 km s^{-1} in the continental upper and lower crust (Husen et al., 2000; Oncken et al., 2003; Krabbenhöft et al., 2004). A range of density values for the sediments were obtained from P-wave velocity of the continental margin (2.0 – 4.5 km s^{-1}; Husen et al., 2000; Krabbenhöft et al., 2004).

The geometric configuration and density structures of the slab and overriding continental lithosphere were constrained by seismic tomography and receiver function. The velocities of the oceanic and continental lithospheric mantle range from 7.8 to 8.15 km s^{-1} and from 7.6 to 8.1 km s^{-1}, respectively (Norabuena and Snoke, 1994; Oncken et al., 2003; Krabbenhöft et al., 2004). The density of the asthenosphere is based on P-wave travel time model (Norabuena and Snoke, 1994).

The P-wave velocity structures of the Central Andes were converted to their respective densities at relevant pressure and temperature conditions using empirical P-wave velocity–density relation following the Sobolev & Babeyko approach (Sobolev & Babeyko, 1994).

The 2.5-D gravity model was developed using GM-SYS Gravity and Magnetic Modelling software which makes use of Green's theorem to calculate the gravity anomalies of irregular structures. A finite strike length of 100 m has been used on each side of the gravity profile. The densities of the tectonic units are constant along the strike. To improve the fit of the observed gravity to predicted, density values were inverted using ridge-regression algorithm. The errors in the misfit were minimized in a least-square sense. The density values of the final gravity model are shown in Fig. 4. The standard deviation of the final density values is in the order of ± 25 kg m^{-3}.

5 Results and Discussions

5.1 Lithospheric Structure

Geodetic data and models, based on continuous Differential GPS measurements, indicate a highly coupled plate interface in the Central Andes subduction zone (Chlieh et al., 2011; Béjar-Pizarro et al., 2013; Métois et al., 2013). To assess the coupling mechanism of the plate interface between the subducting Nazca slab and the overriding South American plate, a 2.5-D gravity model was developed along 19° S (Fig. 4). The model shows the crust and upper mantle structure of the central segment of the subduction zone. The observed long-wavelength gravity anomalies in the Central Andes are well explained in terms of a subducting Nazca slab along the Peru-Chile trench and a highly segmented fore-arc in the crust and upper mantles structures. The Nazca slab exhibits variable density with depth. The densities range from 2900 to 3200 kg m^{-3} in the oceanic crust and from 3200 to 3360 kg m^{-3} in the lithospheric mantle. The variation of density with depth is due to dehydration and densification of the subducting oceanic lithosphere. The reaction within lithospheric mantle involves breakdown of serpentinite into olivine, orthoclase, and release of water from the slab.

As shown in Fig. 4, the dip of the slab changes along latitudinal line from 37 degree near the trench to 46 degree far from the trench in the fore-arc. The shallow subduction, adjacent to the trench (approximately between 70° and 72° longitude), may have increased the contact area between the subducting and overriding plates and resulted in more compressional stresses in the fore-arc closer to the trench (cf. e.g. Lallemand et al., 2005). The high compressive stresses, due to shallow slab near the trench, may have contributed to plate coupling in the Central Andes. This is in addition to the latitudinal variations of plate coupling attributed to changes in subduction angle.

The crustal structure of the overriding South American plate is segmented much like the subducting Nazca slab. The crustal thickness in the Central Andes increases with increasing elevation from Central to Eastern Cordillera. The maximum crustal thickness in the Central Andes (ca. 50 km) was observed below Altiplano and Eastern Cordillera (Fig. 4). This might be attributed to crustal thickening in the overriding plate that responds to the on-going convergence of the Nazca and South American plates.

The short-wavelength anomalies over the ocean and fore-arc are attributed to crustal heterogeneity at shallow depths (Fig. 4) and could not be modelled due to lack of information.

5.2 Plate Coupling & Asperity Generation

The densities of the upper and lower crust in the fore-arc (2970 – 3000 kg m^{-3}) are much higher than the average density of continental crust (Fig. 4). This is in agreement with results of P-wave tomography of the Central Andes (Fig. 5; Husen et al., 2000). The P-wave tomography of the central Andean subduction zone images the presence of high V_P anomalies (> 7.0 km/s) in the lower crust of the overriding South American plate (Fig. 5; Husen et al., 2000).

The high density and high V_P anomalies are interpreted as remnants of magmatic intrusions and correlate with plutonic outcrops on the surface (cf. e.g. Husen et al., 2000; Schaller et al., 2015). The anomalous fore-arc structures could be batholites or ophiolites emplaced onto continental crust. Previous studies documented the presence of ophiolites in the basement of the southern segment of South America (cf. e.g. Ramos et al., 2000). However, the existence of ophiolites in the Central Andes is not well known. Castroviejo et al (2010) reported the emplacement of ophiolites in the central Peruvian Andes in Eastern Cordillera. Thus, the high-density fore-arc structures, shown in the gravity and velocity models of the Central Andes, could be ophiolites emplaced onto continental crust.

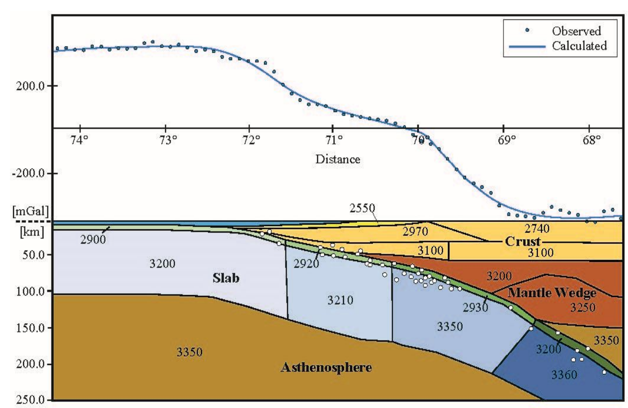

Figure 4: 2.5-dimensional (2.5-D) gravity model of the Central Andes subduction zone along 19° S. The numbers in the model are densities in kg m^{-3}. The white circles are earthquake hypocenters (events from 1957 - 2018).

The high density fore-arc structures in the Central Andes and buoyancy forces may be exerting pressure on the subducting slab and lock the plate interfaces between the overriding and subducting plates. Thus, the along-strike segmentation of the overriding South American plate (crustal thickness and density variations) may be the controlling factor of plate coupling and asperity generation (regions of high seismic moment). The presence of high-density structures in the upper and lower crust resulted in lithostatic load variations in the fore-arc. Figure 6 shows the variations of vertical stress on top of the subducting Nazca slab along East-West transect. The vertical stress anomalies, which are based on density model, are determined relative to a reference lithospheric column. The reference lithospheric column represents the average structures of continental crust and upper mantle and consists of 15 km thick upper crust, 20 km thick lower crust, and lithospheric mantle. The densities of the reference upper crust, lower crust and lithospheric mantle are 2670, 2900, and 3350 kg m^{-3}, respectively.

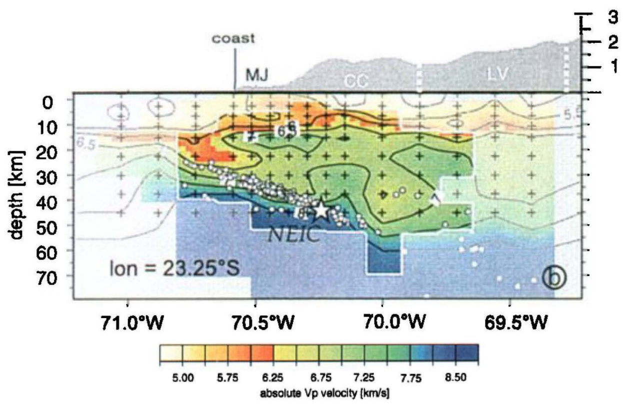

Figure 5: P-wave velocity tomography of Central Andes (Husen et al., 2000). The vertical section shows the presence of high P-wave velocity anomalies (> 7.0 km/s) in the lower crust of the overriding South American plate. White circles are hypocenters. Star marks the hypocenter of the 1995 Antofagasta earthquake. Abbreviations: CC, Coastal Cordillera; LV, Longitudinal Valley; MJ, Mejillones Peninsula.

As shown in Fig. 6, the fore-arc, where the high-density crustal structures are present, is characterized by positive vertical stress anomalies. The anomalies range from 8.7 MPa near the trench to 34.6 MPa in the fore-arc. This indicates that the high-density fore-arc structures may be exerting pressure on the subducting Nazca slab.

6 Conclusions

Geodetic measurements and seismological studies in the Central Andes indicate a highly coupled plate interface between the subducting Nazca and overriding South American plates. The convergent zone is accumulating elastic energy and building up stresses. The present study assessed the locking mechanism of plate interfaces in the

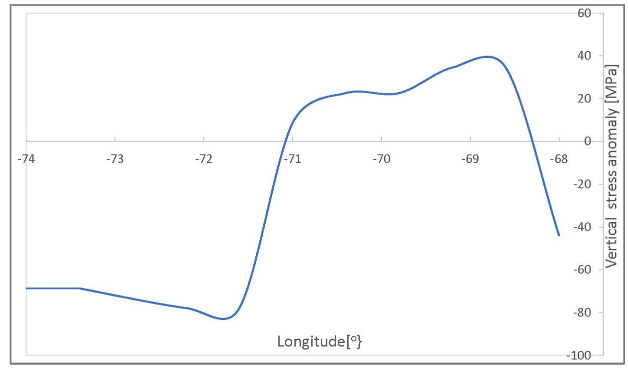

Figure 6: Vertical stress anomalies on top of the subducting Nazca plate along East-West transect at 19° S.

Central Andes based on gravity data modelling. The gravity model provided a possible explanation of plate coupling that resulted in seismic gap zones in the Central Andes. The Gravity model indicates that the densities of the fore-arc in the upper and lower crust are significantly higher than the average density of continental crust. The high density fore-arc structure in the continental crust and Bouyancy force may have exerted pressure on the Nazca slab and locked the plate interfaces beneath the Central Andes subduction zone. Thus, the trench-parallel crustal thickness and density variations in the Central Andes may control plate coupling and asperity generation. The high compressive streses near the trench, due to shallow subduction, may have contributed to the interseismic coupling in the Central Andes.

The present study does not include other possible factors that control plate coupling and asperity generation. Seafloor roughness and variations in pore-fluid pressure may control plate coupling and asperity generation in the Central Andes (Delouis et al., 1996; Bilek et al., 2003; Bilek, 2007; Bassett and Watts, 2015). An increased pore-fluid pressure in sediments along subduction channel can reduce normal stress and hinder elastic strain accumulation (Delouis et al., 1996; Tassara, 2010). I leave a more detailed evaluation of the effects of Seafloor roughness and pore-fluid pressure on plate coupling for future studies.

Acknowledgement: This work has been supported by CARSCA (College Academy of Research, Scholarship, and Creative Activity, a unit of the College of Arts and Sciences, The University of Alabama). The author thanks Carla Braitenberg and an anonymous reviewer for their thoughtful and constructive comments, which were of great help in the preparation of the final version of this paper.

References

Allmendinger, R., W., Jordan, T. E., Kay, S. M., and Isacks, B. L., 1997. The evolution of the Altiplano-Puna Plateau of the Central Andes, Annu. Rev. Earth Planet. Sci., 25,139–174.

Amante, C. and Eakins, B.W., 2009. ETOPO1 1 arc-minute global relief model: Procedures, data sources and analysis, US Department of Commerce, National Oceanic and Atmospheric Administration, National Environmental Satellite, Data, and Information Service, National Geophysical Data Center, Marine Geology and Geophysics Division, 19.

Álvarez, O., Gimenez, M.E., Braitenberg, C., and Folguera A., 2012. GOCE satellite derived gravity and gravity gradient corrected for topographic effect in the South Central Andes region. Geophys. J. Int., 190, 2, 941-959. doi:10.1111/j.1365-246X.2012.05556.x

Álvarez, O., Nacif, S., Gimenez, M., Folguera, A, and Braitenberg, C., 2014. GOCE derived vertical gravity gradient delineates great earthquake rupture zones along the Chilean margin, Tectonophysics, 622, 198–215, doi:10.1016/j.tecto.2014.03.011.

Álvarez, O., Pesce, A., Gimenez, M., Folguera, A. Soler, S., and Chen, W., 2017. Analysis of the Illapel Mw=8.3 thrust earthquake rupture zone using GOCE derived gradients. Pure and Applied Geophysics, 174 (1) 47-75. https://doi.org/10.1007/s00024-016-1376-y

Anderson, M. L., Alvarado, P., Zandt, G., and Beck, S., 2007.Geometry and brittle deformation of the subducting Nazca plate, central Chile and Argentina. Geophys. J. Int., 171(1), 419–434, doi:10.1111/j.1365-246X.2007.03483.x.

Audin, L., P. Lacanb, P., Tavera, H., and Bondoux, F. 2008. Upper plate deformation and seismic barrier in front of Nazca subduction zone: The Chololo fault system and active tectonics along the coastal cordillera, southern Peru. Tectonophysics, 459(1-4), 174-185, doi:10.1016/j.tecto.2007.1011.1070.

Bassett, D. and Watts, A.B., 2015. Gravity anomalies, crustal structure, and seismicity at subduction zones: 1. Seafloor roughness and subducting relief. Geochemistry, Geophysics, Geosystem, 1508–1540, http://dx.doi.org/10.1002/2014GC005684.

Béjar-Pizarro, M., Socquet, A., Armijo, R., Carrizo, D., Genrich, J., and Simons, M., 2013. Andean structural control on interseismic coupling in the North Chile subduction zone, Nat. Geosci., 6, 462–467, doi:10.1038/NGEO1802.

Bilek, S. L., 2010. Seismicity along the South American subduction zone: Review of large earthquakes, tsunamis, and subduction zone complexity, Tectonophysics, 495 (1-2), 2–14, doi:10.1016/j.tecto.2009.02.037.

Bilek, S.L., 2007. Influence of subducting topography on earthquake rupture. In: Dixon, T., Moore, J.C. (Eds.), The Seismogenic Zone of Subduction Thrust Faults. Columbia University Press.

Bilek, S.L., Schwartz, S.Y., and DeShon, H.R. 2003. Control of seafloor roughness on earthquake rupture behavior. Geology, 31 (5): 455-458.

Bomfim, E. P., Braitenberg, C., and Molina, E. C., 2013. Mutual evaluation of global gravity models (EGM2008 and GOCE) and terrestrial data in Amazon Basin, Brazil. Geophys. J. Int, vol. 195, 870 - 882, ISSN: 1365-246X, doi: 10.1093/gji/ggt283.

Braitenberg, C. and Rabinovich, A.B., 2017. The Chile-2015 (Illapel) Earthquake and Tsunami. Pure and Applied Geophysics Topical Volume series, Birkhäuser; 1st ed., pp348.

Comte, D., Battaglia, J., Thurber, C., Zhang, H., Dorbath, L., and Glass, B., 2004. High-resolution subducting slab structure beneath northern Chile using the double-difference tomography method. Eos Trans. AGU 85 (47), Fall Meet. Suppl., Abstract S53B-0200.

Castroviejo, R., Rodrigues, J.F., Tassinari, C., Pereira, E, and Acosta, J., 2010. Ophiolites in the Eastern Cordillera of the central Peruvian Andes. IMA2010 Cogress. 20th General Meet. Internt. Mineralogical Associ, Acta Mineral Petrgr., abstract Ser. Szeged, Budapest.

Cella, F., 2015. GTeC- A versatile MATLAB tool for a detailed computation of the terrain correction and Bouguer gravity anomalies. Computer and Geosciences, 84, 72-85.

Charrier, R., Hérail, G., Pinto, L., García, M., Riquelme, R., Farías, M., and Muenoz, N., 2013. Cenozoic tectonic evolution in the Central Andes in northern Chile and west-central Bolivia: implications for paleogeographic, magmatic and mountain building evolution. Int. J. Earth Sci. (Geol. Rundsch) 102 (1), 235–264, http://dx.doi.org/10.1007/s00531-012-0801-4, 10.1007/s00531-012-0801-4.

Chlieh, M., Perfettini, H., Tavera, H., Avouac, J.-P., Remy, D., and Nocquet, J.-M., 2011. "Interseismic coupling and seismic potential along the Central Andes subduction zone". J. Geophys. Res., 116, B12405, doi:10.1029/2010JB008166, 2011.

Delouis, B., Cisternas, A., Dorbath, L., Rivera, L., and Kausel, E., 1996. The Andean subduction zone between 22 and 25S (northern Chile): precise geometry and state of stress. Tectonophysics 259 (1–3), 81–100, http://dx.doi.org/10.1016/0040-1951(95)00065-8.

Förste, C., Bruinsma, S.L., Shako, R., Marty, J.C., Flechtner, F., Abrikosov, O., Dahle, C., Lemoine, J.M., Neumayer, K.H., Biancale, R., Barthelmes, F., König, R., and Balmino, G.; 2011. EIGEN-6 - A new combined global gravity field model including GOCE data from the collaboration of GFZ-Potsdam and GRGS-Toulouse. Geophysical Research Abstracts, Vol. 13, EGU2011-3242-2, EGU General Assembly, Vienna.

Förste, C., Bruinsma, S., Abrykosov, O., Flechtner, F., Marty, J.-C., Lemoine, J.-M., Dahle, C., Neumayer, K.-H., Barthelmes, F., König, R., and Biancale, R. 2014. EIGEN-6C4 - The latest combined global gravity field model including GOCE data up to degree and order 1949 of GFZ Potsdam and GRGS Toulouse. Geophysical Research Abstracts, Vol. 16, EGU2014-3707, General Assembly European Geosciences Union, Vienna,

Gutknecht, B.D., Götze, H.-J., Jentzsch, G., Jahr, T., Mahatsente, R., and Zeumann, S., 2014. Structure and state of stress of the Chilean subduction zone from terrestrial and satellite-derived gravity and gravity gradient data. Surveys in Geophysics, DOI: 10.1007/S10712-014-9296-9.

Gutscher, M.-A., Spakman, W., Bijwaard, H., and Engdahl, R., 2000. Geodynamics of flat subduction: Seismicity and tomographic constraints from the Andean margin. Tectonics, 19, 814–833.

Goetze, H.J., Lahmeyer, B, Schmidt, S., and Strunk., S., 1994. The lithospheric structure of the Central Andes (20–26S) as inferred from interpretation of regional gravity. In: Reutter KJ, Scheuber E, Wigger PJ (eds) Tectonics of the Southern Central Andes—structure and evolution of an active continental margin. Springer, Berlin.

Goetze, H.J. and Pail, R., 2018. Insights from recent gravity satellite missions in the density structure of continental margins – With focus on the passive margins of the South Atlantic. Gondwana Research, 53, 285 – 308.

Hackney, R., Echtler, H., Franz, G., Goetze, H.-J., Lucassen, F., Marchenko, D., Melnick, D., Meyer, S.S., Tasárová, Z., Tassara, A., and Wienecke, S., 2006. The segmented overriding plate and coupling at the south-central Chile margin (36S–42S). In: Oncken, O., Chong, G., Franz, G., Giese, P., Goetze, H.-J., Ramos, V.A., Strecker, M., Wigger, P. (Eds.), The Andes – Active Subduction Orogeny. Frontiers in Earth Science Series, vol. 1. Springer-Verlag, Berlin/Heidelberg/New York, 355–374.

Hosse, M., Pail, R., Horwath, M., Holzrichter, N., and Gutknecht, B.D., 2014. Combined Regional Gravity Model of the Andean Convergent Subduction Zone and Its Application to Crustal Density Modelling in Active Plate Margins. Surv. Geophys., 35, 1393 – 1415.

Husen, S., Kissling, E., and Flueh, E.R., 2000. Local earthquake tomography of shallow subduction in north Chile: a combined onshore and offshore study. J. Geophys. Res. Solid Earth (1978-2012.

Isacks, B., 1988. Uplift of the central Andean plateau and bending of the Bolivian orocline. J. Geophys. Res., 93, pp.3211-3231.

Jarvis, A., Reuter, H.I., Nelson, A., and Guevara, E., 2008. Hole-filled SRTM for Globe Version 4: The CGIAR-CSI SRTM 90m Database: http://srtm.csi.cgiar.org (accessed March 2016).

Kato, A. and Nakagawa, S., 2014. Multiple slow-slip events during a foreshock sequence of the 2014 Iquique, Chile Mw 8.1 earthquake. Geophys. Res. Lett., 41, 5420–5427, doi:10.1002/2014GL061138.

Krabbenhöft, A., Bialas, J, Kopp, H., Kukowsky, N., and Huebscher, C., 2004. Crustal structure of the Peruvian continental margin from wide angle seismic studies. Geophys. J. Int., 159, 749– 764.

Koether, N., Goetze, H.J., Gutknecht, B.D., Jahr, T., Jentzsch, G., Luecke, O.H., Mahatsente, R., Sharma, R., and Zeumann, S., 2012. The seismically active Andean and Central American margins: can satellite gravity map lithospheric structures? J. Geodyn. 59–60:207–218. doi:10.1016/j.jog.2011.11.004.

Lallemand, S., Heuret, A., and Boutelier, D., 2005. On the relationships between slab dip, back-arc stress, upper plate absolute motion, and crustal nature in subduction zones, Geochem. Geophys. Geosyst., 6, 1525-2027, Q09006, doi:10.1029/ 2005GC000917.

Li, B. and Ghosh, A., 2016. Imaging Rupture Process of the 2015 Mw 8.3 Illapel Earthquake Using the US Seismic Array. Pure Appl. Geophys. 173, 2245-2255

Mayer-Gürr, T., Rieser, D., Höck, E., Brockmann, J. M., Schuh, W. D., Krasbutter, I., Kusche, J., Maier, A., Krauss, S., Hausleitner, W., Baur, O., Jäggi, A., Meyer, U., Prange, L., Pail, R., Fecher, T., and Gruber, T., 2012. The new combined satellite only model GOCO03s. International Symposium on Gravity, Geoid and Height Systems (GGHS2012), Abstract.

Métois, M., Socquet, A., Vigny, C., Carrizon, D., Peyrat, S., Delorme, A., Maureira, E., Valderas-Bermejo, M.-C., and Ortega, I., 2013. Revisiting the North Chile seismic gap segmentation using GPS-derived interseismic coupling. Geophys. J. Int., 194, 1283–1294, doi:10.1093/gji/ggt183.

Moreno, M., Melnick, D., Rosenau, M., Bolte, J., Klotz,J., Echtler,H., Baez, J., Bataille,K., Chen, J., Bevis, M., Hase, H., and Oncken, O., 2011. Heterogeneous plate locking in the South–Central Chile subduction zone: Building up the next great earthquake. Earth and Planetary Science Letters, 305(3-4), 413–424, doi:10.1016/j.epsl.2011.03.025

Moreno, M. S., Bolte, J. Klotz, J., and Melnick, D., 2009. Impact of megathrust geometry on inversion of coseismic slip from geodetic data: Application to the 1960 Chile earthquake. Geophysical Research Letters, 36(16), doi:10.1029/2009gl039276

Moreno, M. S., Klotz, J., Melnick, D., Echtler, H., and Bataille, K., 2008. Active faulting and heterogeneous deformation across a megathrust segment boundary from GPS data, south central Chile (36-39°S). Geochemistry, Geophysics, Geosystems, 9(12), n/a–n/a, doi:10.1029/2008gc002198.

Norabuena and Snoke, 1994. Structure of the subducting Nazca Plate beneath Peru. Journal of Geophysical Research, Vol. 99, NO. B5, PAGES 9215-9226

Oncken, O., Asch, G., Haberland, C., Metchie, J., Sobolev, S., Stiller, M., Yuan, X.,Brasse, H., Buske, S., Giese, P., Goetze, H.J., Lueth, S., Scheuber, E., Shapiro, S.,Wigger, P., Yoon, M.-K., Bravo, P., Vieytes, H., Chong, G., Gonzales, G., Wilke, H.-G., Lüschen, E., Martinez, E., Rössling, R., Ricaldi, E., and Rietbrock, A., 2003. Seismic imaging of a convergent continental margin and plateau in the central Andes (Andean Continental Research Project 1996 (ANCORP'96), J. Geophys. Res. 108 (B7), 2328, http://dx.doi.org/10.1029/2002JB001771.

Oncken, O., Chong, G., Franz, G., Giese,. P., Götze, H-J., Ramos, V., Strecker, M., and Wigger, P., 2006. The Andes – Active Subduction Orogeny. Frontiers in Earth Science Series, Vol 1. Springer-Verlag, Berlin Heidelberg New York, 567pp.

Pavlis, N.K., Holmes, S.A., Kenyon, S.C., and Factor, J.K., 2012 . The development and evaluation of the Earth Gravitational Model 2008 (EGM2008),. J. Geophys Res 117(B4), doi:10.1029/2011JB008916.

Prezzi, C., Goetze, H.J., and Schmidt, S., 2009. 3D density model of the Central Andes. Phys Earth Planet Inter. 177(3–4):217–234. doi:10.1016/j.pepi.2009.09.004

Pérez-Gussinyé, M., Lowry, A. R., Phipps Morgan, J. and Tassara, A., 2008. Effective elastic thickness along the Andean margin and their relationship to subduction geometry. Geochem. Geophys. Geosyst., 9 (2).

Ramos, V.A., Escayola, M., Mutti, D., and Vujovich, G., 2000. Proterozoic–early Paleozoic ophiolites of the Andean basement of southern South America. Geological Society of America Special Paper 349, 331-349.

Rietbrock, A., Ryder, I ., Hayes, G., Haberland, C., Comte, D., Roecker, S., and Lyon-Caen., H., 2012. Aftershock seismicity of the 2010 Maule Mw=8.8, Chile, earthquake: Correlation between coseismic slip models and aftershock distribution? Geophys. Res. Lett., Vol. 39, L08310, doi:10.1029/2012GL051308.

Ruiz. S and Madariaga, R., 2018. Historical and recent large megathrust earthquakes in Chile. Tectonophysics, 733, 37-56

Schaller, T., Andersen,J., Götze, H.-J.,Koproch,N., Schmidt,S., Sobiesiak,M, Splettstoeßer, S., 2015. Segmentation of the Andean margin by isostatic models and gradients. Journal of South American Earth Sciences, 59, pp.69-85.

Schmidt, S., Goetze, H.J., 2006. Bouguer and isostatic maps of the Central Andes. In: Oncken, O., Chong, G., Franz, G., Giese, P., Goetze, H.J., Ramos, V.A., Strecker, M., Wigger, P. (Eds.), The Andes – Active Subduction Orogeny. Frontiers in Earth Science Series, vol. 1. Springer-Verlag, Berlin/Heidelberg/New York, pp. 559–565

Schurr, B. G. Asch, G., Rosenau, M., Wang, R., Oncken, O., Barrientos, S., Salazar, P.,

Sobiesiak M., Meyer, U., Schmidt, S., Götze, H-J. and Krawczyk, C. M., 2007. Asperity generating upper crustal sources revealed by b value and isostatic residual anomaly grids in the area of Antofagasta, Chile. J. Geophys. Res., 112, B12308, doi:10.1029/2006JB004796.

Sobolev, S.V., Babeyko, A.Y., 1994. Modeling of mineralogical composition,density, and elastic wave velocities in anhydrous magmatic rocks. Surv.Geophys. 15, 515–544.

Tassara , A., 2005. Interaction between the Nazca and South American plates and formation of the Altiplano–Puna plateau: Review of a flexural analysis along the Andean margin (15°–34°S), Tectonophysics 399, pp.39-57.

Tassara, A., Götze, H-J., Schmidt, S. and Hackney, R., 2006. Three-dimensional density model of the Nazca plate and the Andean continental margin, J. Geophys. Res. 111, Nr. B9, B09404, doi:10.1029/2005JB003976.

Tassara, A., 2010. Control of forearc density structure on megathrust shear strength along the Chilean subduction zone, Tectonophysics 495:34-47. doi: 10.1016/j.tecto.2010.06.004.

Yáñez , G., Ranero, C.R., von Huene, R., Diaz, J., 2001. Magnetic anomaly interpretation across the southern central Andes (32–34): the role of the Juan Fernañdez Ridge in the late Tertiary evolution of the margin, J. Geophys. Res.106, 6325–6345.

Yi, W., Rummel, R., 2013. A comparison of GOCE gravitational models with EGM2008. Journal of Geodynamics, Vol. 73, 14-22, DOI: 10.1016/j.jog.2013.10.004.

Yuan, X., Sobolev, S. V., Kind, R., Oncken, O., Bock, G., Asch, G., Comte, D., 2000. Subduction and collision processes in the Central Andes constrained by converted seismic phases. Nature, 408(6815), 958–961. http://doi.org/10.1038/35050073